Electron transport through π-stacked molecular multilayers: Metal-semiconductor transition

Sergey V. Faleev* and François Léonard
Sandia National Laboratories, Livermore, California 94551, USA
(Received 30 May 2007; revised manuscript received 1 August 2007; published 20 September 2007)

We present a theoretical study of electron transport in π-stacked polythiophene multilayers (with varying number of layers L) sandwiched between Au(111) electrodes in a geometry of flat molecular layers lying parallel to the electrode surface, as suggested by recent experiments. We use a method based on the local density approximation of density functional theory and implemented in the framework of the tight-binding linear muffin-tin orbital approach in its atomic sphere approximation. A fully atomistic description of the electrodes and the nanosystem is used, and the self-consistent charge and electrostatic potential for the system under applied bias are calculated using the nonequilibrium Green's function approach. For a small number of layers, metal-induced gap states render the molecular film metallic, while for thicker films, the conductance decreases exponentially with the number of layers, $\sigma \approx G_0 \exp[-0.81(L-3.4)]$, indicating semiconductorlike behavior; the transition between these two regimes occurs at a film thickness of 20 Å ($L \approx 6$). This length scale originates from the decay length of the gap states (4.24 Å) and the "band bending" in the multilayer. For $L=1$, the current depends linearly on applied voltage, while at $L>1$, current is nonlinear, reflecting strong bias and energy dependence of the transmission function due to formation of the band gap near the Fermi energy.

DOI: 10.1103/PhysRevB.76.125108 PACS number(s): 72.10.−d, 73.63.Rt, 85.65.+h

I. INTRODUCTION

Thin films of semiconducting polymers have been studied as promising materials for many technological applications,[1–7] including organic light emitting devices, thin film transistors, photovoltaic devices, and sensors. Important factors in these applications are the efficiency of charge injection at organic/metal interfaces and the subsequent charge transport through the polymeric films. Addressing these issues requires a fundamental understanding of the electronic structure of organic/metal interfaces and of transport of electrons through stacks of molecular layers.

In the present paper, we use nonequilibrium *ab initio* calculations to study the electronic transport properties of ultrathin polythiophene films in contact with metals, for which the structure is well understood experimentally. Poly- and oligothiophene thin films are attractive because they have good chemical stability and, among organic materials, excellent electrical transport properties due to the π-electron system delocalized along the one-dimensional polymer backbone. Very clean films can be fabricated ranging from a single monolayer to thick films, and their properties can be chemically tuned for specific applications.[5–10] While much work has focused on hopping transport through disordered polymeric films at high temperatures, electronic transport through ultrapure well-ordered polymeric films at lower temperatures occurs in the band regime instead.[11] This regime is the focus of the present paper.

It has been experimentally shown[10,12–15] that thin oligothiophene films form flat molecular layers parallel to metal surfaces, and such order is stable in a range from a few[10] and up to 12 layers.[13] Central questions for charge injection and transport are as follows: What is the impact of the metal on the electronic structure of the polythiophene? What is the band alignment near and far from the organic/metal interface? What are the important length scales determining the properties of the thin films, and what is their origin? What is the conductance of such films, and how does it depend on the film thickness?

To answer these questions, we consider a system of polythiophene (PT) flat layers (with number of layers, $L=1,2,\ldots,12$) arranged parallel to the (111) gold electrodes (see Fig. 1 for unit cell of the system with $L=2$). Thus, we study electron transport in the direction perpendicular to the thiophene rings (z axis in Fig. 1). We note that although semiempirical[16,17] and *ab initio*[18] approaches have been used to calculate the conductance of molecules with varying lengths, all of these studies were performed for molecules attached by both ends to electrodes, with current flowing in the plane of the molecule. The present study investigates the dependence of conductance on the number of layers of molecules arranged in planes parallel to the electrode surface, with current flowing perpendicular to the molecular plane.

The paper is organized as follows. In Sec. II, we describe the method used. In Sec. III, we present computational details. In Sec. IV, we present the transmission functions at different bias voltages and different numbers of layers and current-voltage characteristics of the system and discuss the results. Conclusions are presented in Sec. V.

II. THEORETICAL METHOD

By nature, a first-principles quantum-mechanical approach is necessary for calculation of the transmission coefficient $T(E)$ and current-voltage (I-V) curve of a nanosystem because quantum effects dominate the transport properties at the nanoscale. In this paper, we use the nonequilibrium Green's function (NEGF) approach that we developed and implemented recently[19] based on tight-binding linear muffin-tin orbital method in its atomic sphere approximation (TB-LMTO-ASA).[20] Our approach is an all-electron *ab initio* method that treats electrodes and the nanosystem between the electrodes on the same (fully atomistic) footing. The advantage of the tight-binding formulation of the LMTO-ASA

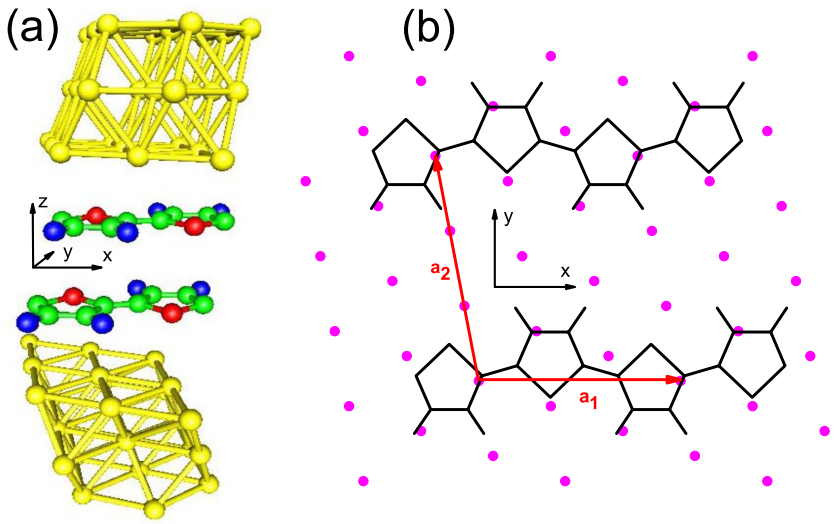

FIG. 1. (Color online) (a) The unit cell for simulation of transport properties of PT layers (illustrated for $L=2$) coupled to two Au (111) surfaces. The cell is repeated in the xy plane. Semi-infinite gold leads (not shown) are attached to the cell. (b) Equilibrium atomic positions in the xy plane of the first PT layer and first layer of gold. Positions of gold atoms are shown by dots; positions of molecular layer atoms are shown by connected lines. $\mathbf{a}_1$ and $\mathbf{a}_2$ are translation vectors of the unit cell in the xy plane. Four xy unit cells are shown.

method is that effectively, only a few nearest neighbor atoms interact with each other, thus making numerical computations very efficient. The CPU runtime scales linearly with the number of molecular layers L.

The system is divided into three regions: the right electrode, the central region, and the left electrode. All charge and electrostatic potential relaxation is assumed to occur inside the central region, which includes a few atomic layers of each physical electrode, while the left and right electrode regions are assumed to have bulk charge distributions and potentials. This condition can be checked by including more metal layers in the central region. Right and left electrodes are assumed to be in thermal equilibrium with chemical potentials μ_R and μ_L, correspondingly, whose difference determines the applied bias $\mu_R-\mu_L=eV$.

In our calculations, we first determine the self-consistent bulk charge density and electrostatic potential distribution for each electrode separately. The local density approximation of the density functional theory is used to define the electrostatic potential. Next, the self-consistent charge density and potential distribution are obtained for the whole system for each applied bias voltage. The transmission function is then calculated, and current is obtained by using the Landauer formula at zero temperature,

$$I(V) = G_0 \int_{\mu_L}^{\mu_R} T(E,V)dE, \tag{1}$$

where $G_0=2e^2/h$ is the quantum of conductance. Here, we show explicitly the dependence of the transmission coefficient $T(E,V)$ on applied voltage V in order to stress that it is calculated for a nonequilibrium open system whose charge density and electrostatic potentials are found self-consistently by using the NEGF technique.[19]

III. COMPUTATIONAL DETAILS

The central region of the system we are interested in consists of three Au(111)-(3×3) layers, the L layers of polythiophene molecules lying parallel to the Au surface, and then three more Au(111)-(3×3) layers. The semi-infinite left and right gold electrodes are attached to the ends of the central region. An example of the central region unit cell with two polythiophene layers is shown on Fig. 1. The cell is assumed to repeat itself periodically in the xy plane along translation vectors $\mathbf{a}_1$ and $\mathbf{a}_2$ as shown in Fig. 2. Note that translation along $\mathbf{a}_1$ produces a chain polythiophene molecule that is infinitely long along the x axis. The gold atoms are assumed to be in their bulk positions. [It has been shown for a benzene dithiol (BDT) molecule attached to the Au(111) surface[19,21,22] that relaxation of gold layers is unimportant for transmission and current calculations.]

Atomic positions of polythiophene molecules and relative positions of the molecules and gold surface were determined as follows. First, we found the equilibrium positions of atoms in a single chain polythiophene molecule by using the VASP molecular dynamics program,[23] assuming that the molecule is flat. Then, with fixed coordinates of atoms inside each molecular layer, we determine the xy shift of molecular planes for adjacent layers and the z distance between the layers by minimizing the total energy in VASP. In this procedure, we keep the y distance between molecular chains within the same layer large enough so the interaction be-

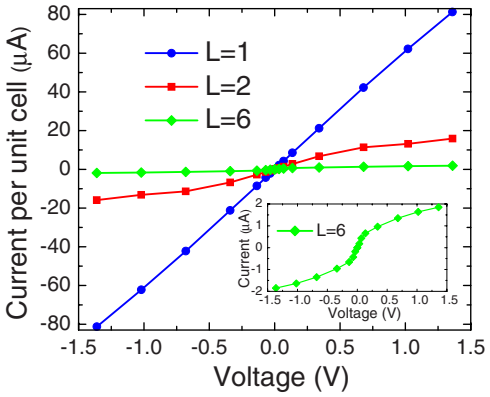

FIG. 2. (Color online) Current as a function of bias voltage for $L=1$, 2, and 6. Inset shows current for $L=6$ in greater detail.

tween different chains in the same layer is negligible. We found that adjacent layers are at equilibrium if they are shifted by 0.81 Å in the x direction and by 1.42 Å in the y direction relative to each other. The equilibrium distance between flat molecular layers equals 3.31 Å, in agreement with the experimental value of 3.3 Å.[13]

Next, we rotate the Au(111) surface in the xy plane in order to map the translation vector of the molecule to the closest translation vector of the Au (111) surface. The translation vector $\mathbf{a}_1$ of the Au(111) surface shown in Fig. 1 is the closest one, with a mismatch of 1.5%. To create a manageable unit cell, we uniformly compress the x coordinates of the PT molecule by 1.5% so that its translation vector along the x axis fits the translation vector $\mathbf{a}_1$ of the Au (111) surface (as shown previously for BDT, such small variations in the atomic positions of the molecule do not affect the results appreciably[19,22]). Translation vector $\mathbf{a}_2$ is chosen in such a way that the unit cell of one Au layer contains nine Au atoms. We found that results for the transmission functions and current do not change significantly if we vary the xy cell size by choosing the $\mathbf{a}_2$ vector such that one Au layer contains seven, eight, or nine Au atoms. We also checked that results do not change appreciably if we include an extra Au layer at each end of the central region.

Finally, we find the xy position of a single molecular layer relative to the Au (111) surface and the z distance between them by minimizing the total energy in VASP. The resulting relative positions of Au atoms and atoms of the molecular layer are shown in Fig. 1. The equilibrium z distance is 3.08 Å. Several other relative xy positions were checked, simulating the shift of the molecular layer relative to the gold surface. It was found that the transmission function at the Fermi energy for such shifts in the case of $L=1$ changes by less than 10% and the overall shape of the function does not change significantly.

The atomic sphere approximation assumes that all space is filled by (overlapping) spheres and that the volume of the interstitial region vanishes. In order to fill the vacuum space between Au electrodes with spheres, we used the Stuttgart LMTO-ASA program.[24] This program fills space by empty spheres using the following criteria: the sum of the volume of all spheres should be equal to the volume of all space, the average overlap between the spheres should be minimal, and the radii of all spheres should be chosen in such a way that the spheres overlap in the region close to the local maximum of the electrostatic potential. The choice of the empty sphere packing structure is not unique. This is the main drawback of the ASA when applied to systems that contain large vacuum regions. On the other hand, for a large enough number of closely packed empty spheres, the results only weakly depend on the empty sphere packing structure. In our case, in addition to 54 Au atomic spheres and $14\times L$ polythiophene atomic spheres, we used from 70 to 110 empty spheres per molecular layer to fill the vacuum space in the central region in order to confirm the appropriateness of the empty sphere packing structure.

We use an $n\times n$ grid in the surface Brillouin zone (SBZ), where n is the number of $\mathbf{k}$ points along each translation vector of the SBZ. Our results are well converged for $n=10$ for calculation of the electronic structure. In order to get well converged results for the transmission function, we increase the number of points to $n\approx 40$.

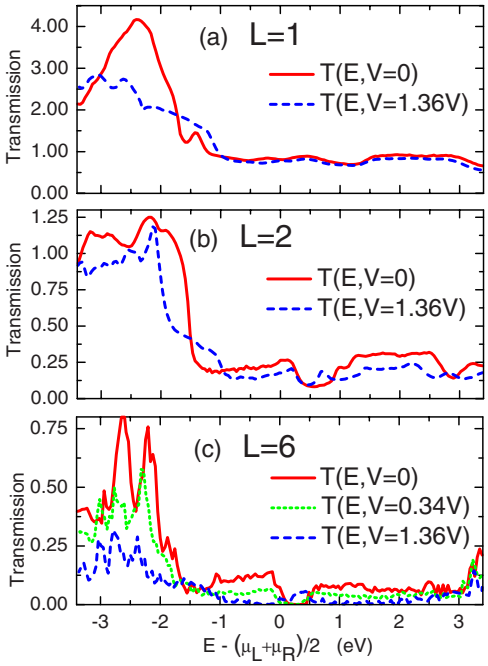

FIG. 3. (Color online) Transmission function for (a) $L=1$, (b) $L=2$, and (c) $L=6$ calculated for bias voltages shown. Note the difference in the vertical scales.

IV. RESULTS AND DISCUSSION

Current-voltage I-V characteristics of the molecular layer were calculated for one, two, and six PT layers for bias voltages ranging from −1.36 to 1.36 V. The I-V curve for these cases are shown in Fig. 2. As the figure indicates, current significantly decreases with increasing number of layers L and qualitatively changes from linear to nonlinear. To explain the origin of this behavior, we consider the transmission probability as a function of energy.

The transmission function for $L=1$ is shown in Fig. 3(a) for 0 and 1.36 V bias. The zero of energy in this figure represents the Fermi energy (E_F), or $(\mu_L+\mu_R)/2$ when finite bias is applied. It is seen that for $L=1$, the transmission function close to E_F is rather featureless: it weakly depends on energy and applied bias. Therefore, the current shown in Fig. 2 for $L=1$ is linear. Since bulk polythiophene is a semiconductor with a 0.5 eV band gap for the studied geometry, the metalliclike behavior of the single PT layer system denotes strong interaction with the gold leads.

The transmission for two molecular layers is shown in Fig. 3(b) as a function of energy for 0 and 1.36 V bias. The band gap of bulk polythiophene is starting to form, as evidenced by the dip in the equilibrium transmission near +0.6 eV. This dip in the equilibrium transmission splits into two dips when a bias voltage is applied. For a 1.36 V bias, the energy difference between the minima of these two dips is ~0.5 eV in correspondence with the ~0.5 V difference of the average induced electrostatic potential between the two

PT layers (the induced potential is a smooth function of the coordinate z, with an almost linear behavior between the gold electrodes, and is well screened in the lead regions).

The calculated I-V curve for $L=2$ shows a nonlinear behavior because the transmission depends more strongly on both the energy and the applied bias compared to the $L=1$ case. For $L=2$, the decrease of the differential conductance with increased voltage in the range from 0.5 to 1 V is explained by a decrease of the transmission away from the small peak near +0.2 eV and also by the general decrease of transmission near E_F with increasing bias. The differential conductance begins to increase at biases above 1 V when a small peak at +0.7 eV begins to enter the integration window of Eq. (1).

The transmission for the $L=6$ system is shown in Fig. 3(c) as a function of energy for 0, 0.34, and 1.36 V bias. The thickness of the PT film is large enough to allow a band gap in the central layers, resulting in a small equilibrium transmission in the energy region from +0.1 to +0.4 eV. The equilibrium transmission strongly depends on energy: it rapidly decreases from a local maximum at −0.15 eV to almost zero at +0.15 eV. Also, the transmission for $L=6$ strongly depends on applied voltage: already at $V=0.34$ V, the transmission near E_F is two times smaller then at zero bias. Such a strong dependence of the transmission near E_F on applied bias is related to the fact that at zero applied bias, E_F is located at the edge of the band gap, where the density of states (DOS) rapidly varies with energy, so the response to applied bias is more pronounced for $L=6$ than for $L=1$ or $L=2$, where the DOS at E_F is smoother. The fast decrease of the transmission near E_F with bias results in strongly nonlinear behavior of the current, with a decreasing differential conductance starting at 0.2 V (see inset in Fig. 2) that corresponds to the characteristic energy scale over which the DOS near E_F changes. The density of states projected on the PT layer closest to the middle of the film for systems with $L=1$, 2, and 6 is shown in Fig. 4 at zero bias voltage. It is seen that the projected density of states (pDOS) as a function of energy is similar to the shape of the transmission function with the band gap formation and shifting of the gap closer to the Fermi energy while going from $L=1$ to $L=6$.

For $L=1$ and $L=2$, the broad peak in the equilibrium transmission in the range from −3 to −1.5 eV corresponds to occupied molecular orbitals broadened by interactions with gold. For $L=6$, this broad peak splits into several narrow peaks because of the presence of inner bulklike layers that weakly interact with the gold leads. When finite bias is applied, different molecular layers are at different electrostatic potentials and the energy levels of molecular states localized inside a layer are shifted in accordance with the average induced potential of the layer. These shifts result in a loss of resonant transmission through the molecular states of all six layers, so the transmission decreases with increase in applied voltage bias as seen in Fig. 3(c).

In order to study the dependence of the conductance $\sigma = G_0 T(E_F, V=0)$ on the number of molecular layers, we calculated the equilibrium transmission in the region near E_F for up to 12 molecular layers. The equilibrium transmission for these L (except $L=1$) is shown in Fig. 5(a) as a function of energy. As the number of layers increases, a band gap is

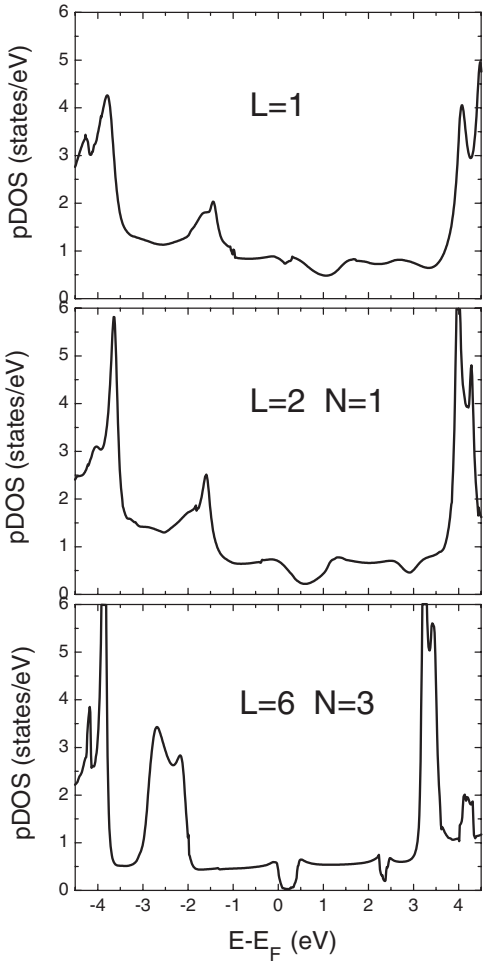

FIG. 4. Density of states projected on the layer closest to the middle of the film as a function of $E-E_F$ for systems with $L=1$, $L=2$, and $L=6$ calculated for zero bias voltages.

formed and the Fermi level is eventually located in this band gap. $L=6$ is roughly the thickness of the PT thin film at which the system makes a transition from two different regimes: a "metallic" regime, where E_F is clearly outside the band gap ($L<5$), and a "semiconducting" regime, where E_F is clearly inside the band gap ($L>7$). The transmission data points from Fig. 5(a) are presented in Fig. 5(b) on a logarithmic scale as a function of L. For a semiconductor, the transmission should depend exponentially on the thickness of the layer, and this is observed for energies in the band gap (e.g., $E=E_F+0.21$ eV) for the PT thin film. However, for the conductance, what matters is the transmission at the Fermi energy: we find that this transmission only obeys an exponential form starting with $L=6$. In a sense, one can say that the PT thin film undergoes a metal-semiconductor transition at $L\approx 6$. A linear fit of $\ln[T(E_F)]$ for $L>6$ is shown in Fig. 5(b) as a dashed line; we obtain the large L asymptotic conductance $\sigma \approx G_0 \exp[-0.81(L-3.4)]$.

To gain a physical picture of the molecular multilayer system, we consider its behavior in terms of a metal/semiconductor/metal system. In such a system, there are two

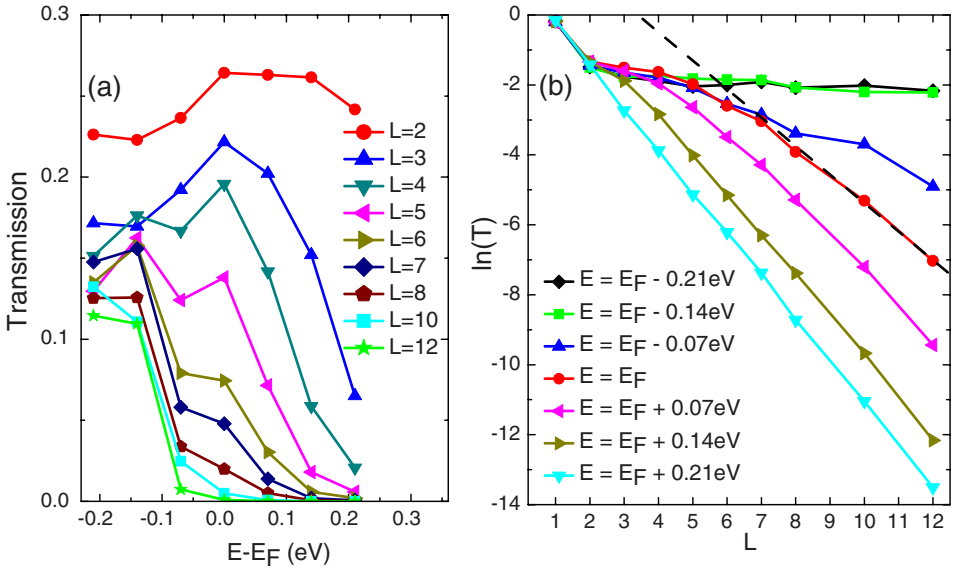

FIG. 5. (Color online) (a) The equilibrium transmission for different L as a function of $E-E_F$. (b) The logarithm of the equilibrium transmission for seven energies near E_F as a function of the number of PT layers L.

length scales that come into play: the decay length of metal-induced gap states (MIGS) and the depletion width (band bending). These two length scales also determine the behavior of the molecular layer system. Indeed, it is clear from Fig. 3(a) that the molecular layer in contact with the metal has essentially no band gap and thus a large density of MIGS; furthermore, Fig. 5(a) indicates that there is a shift of the position of the Fermi level with respect to the band edges for thicker layers, representing the band bending and the depletion width.

Figure 6 shows the deviation ΔV of the potential of the Nth PT layer (calculated in the center of the atomic sphere for each of the 14 atoms of the unit cell) from the potential of an analogous atom in the sixth PT layer for the equilibrium system with $L=12$. It is seen that $\Delta V < 0.04$ eV for N from 3 to 10. Thus, the depletion width is fairly short, about 20 Å; this arises because the Au Fermi level contacts the PT layer in the valence band and creates a large amount of charge near the interface and a sharp band bending.

Because the potential variations are small in the central layers and the Fermi level is in the band gap, the density of states at the Fermi level on each layer is a direct measure of the density of MIGS. To study the MIGS, we calculated the density of states at E_F projected on layer N, pDOS(E_F), for the equilibrium system with $L=12$, as shown in Fig. 6 as a function of N. It is seen that pDOS(E_F) decreases exponentially when N moves away from the metal/PT interface, similar to metal/semiconductor interfaces which normally show decay of MIGS over a characteristic length λ (typically a fraction of a nanometer). By linear fitting of ln[pDOS(E_F)] for $N=3,4,5,6$, we obtain that these states exponentially decrease with increasing distance from the interface with a decay length $\lambda=4.24$ Å.

V. CONCLUSION

We have applied an implementation of the NEGF approach based on the TB-LMTO-ASA method to calculate the transmission and I-V curves of π-stacked molecular thin films sandwiched between metallic electrodes. Our approach is a fully *ab initio* all-electron approach that treats the central region and electrodes on equal footing. This is an application of the *ab initio* approach to study transport properties of a polymer multilayers arranged parallel to the metal surface, as opposed to previously studied systems of a small molecule or oligomer attached at both ends to the electrodes. We found that the molecular layers in contact with the metal strongly interact with the metal, leading to a large density of metal-induced gap states. As the number of molecular layers increases, a band gap opens in the central layers and the Fermi level is positioned in this band gap. The transition to this regime occurs at about six layers, which is also the thickness at which the I-V curve changes from linear to nonlinear, and the transmission becomes exponential. Thus, the molecular film can be thought of as undergoing a metal-semiconductor transition at about 20 Å thickness.

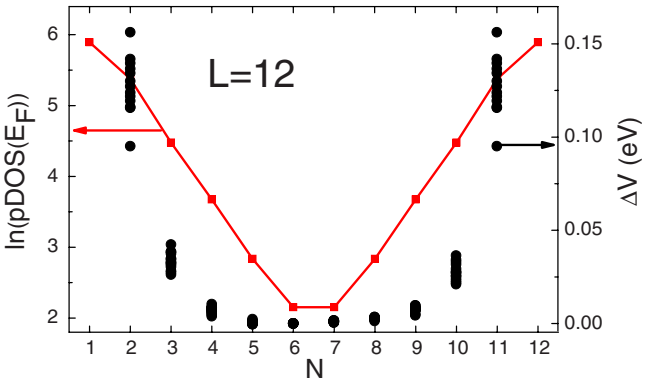

FIG. 6. (Color online) The density of states at the Fermi level projected on layer N for the equilibrium system with $L=12$ (connected squares, left scale) and the deviation of the potential for each of the 14 atoms of the unit cell from the potential of an analogous atom in the sixth PT layer (circles, right scale).

ACKNOWLEDGMENTS

We would like to thank Mark van Schilfgaarde for providing the equilibrium TB-LMTO code on which our nonequilibrium code is based and David Robinson for valuable discussions. Sandia is a multiprogram laboratory operated by Sandia Corporation, a Lockheed Martin Company, for the United States Department of Energy under Contract No. DE-AC04-94-AL8500.

*sfaleev@sandia.gov

[1] C. Adachi, S. Tokito, T. Tsutsu, and S. Saito, Jpn. J. Appl. Phys., Part 2 **27**, L629 (1988).
[2] G. Tourillon and F. Garnier, J. Electrochem. Soc. **130**, 2042 (1983).
[3] S. Miyauchi, T. Dei, I. Tsubata, and Y. Sorimachi, Synth. Met. **41**, 1155 (1991).
[4] G. Horowitz, X. Z. Peng, D. Fichou, and F. Garnier, Synth. Met. **51**, 419 (1992).
[5] G. Horowitz, X. Z. Peng, D. Fichou, and F. Garnier, J. Appl. Phys. **67**, 528 (1990).
[6] S. Hotta and K. Waragai, Adv. Mater. (Weinheim, Ger.) **5**, 896 (1993).
[7] H. Neureiter, W. Gebauer, C. Vaterlein, M. Sokolowski, and E. Umbach, Synth. Met. **67**, 173 (1994).
[8] E. Umbach, C. Seidel, J. Taborski, R. Li, and A. Soukopp, Phys. Status Solidi B **192**, 389 (1995).
[9] W. Gebauer, C. Vaterlein, A. Soukopp, M. Sokolowski, and E. Umbach, Thin Solid Films **284**, 576 (1996).
[10] R. Li, P. Bauerle, and E. Umbach, Surf. Sci. **331**, 100 (1995).
[11] N. Karl, Synth. Met. **133**, 649 (2003).
[12] A. Soukopp, C. Seidel, R. Li, M. Bassler, M. Sokolowski, and E. Umbach, Thin Solid Films **284**, 343 (1996).
[13] W. Gebauer, M. Bassler, A. Soukopp, C. Vatelein, R. Fink, M. Sokolowski, and E. Umbach, Synth. Met. **83**, 227 (1996).
[14] W. Gebauer, M. Bassler, R. Fink, M. Sokolowski, and E. Umbach, Chem. Phys. Lett. **266**, 177 (1997).
[15] A. Soukopp, K. Glockler, P. Kraft, S. Schmitt, M. Sokolowski, E. Umbach, E. Mena-Osteritz, P. Bauerle, and E. Hadicke, Phys. Rev. B **58**, 13882 (1998).
[16] M. Magoga and C. Joachim, Phys. Rev. B **56**, 4722 (1997); **57**, 1820 (1998).
[17] T. Tada, D. Nozaki, M. Kondo, S. Hamayama, and K. Yoshizawa, J. Am. Chem. Soc. **126**, 14182 (2004).
[18] Z. Crljen, A. Grigoriev, G. Wendin, and K. Stokbro, Phys. Rev. B **71**, 165316 (2005).
[19] S. V. Faleev, F. Léonard, D. A. Stewart, and M. van Schilfgaarde, Phys. Rev. B **71**, 195422 (2005).
[20] M. van Schilfgaarde and W. R. L. Lambrecht, in *Tight-Binding Approach to Computational Material Science*, edited by L. Colombo, A. Gonis, and P. Turchi, MRS Symposia Proceedings No. 491 (Materials Research Society, Pittsburgh, 1998).
[21] K. Stokbro, J. Taylor, M. Brandbyge, J. L. Moroz, and P. Ordejon, Comput. Mater. Sci. **27**, 151 (2003).
[22] M. Brandbyge, J. L. Mozos, P. Ordejon, J. Taylor, and K. Stokbro, Phys. Rev. B **65**, 165401 (2002).
[23] G. Kresse and J. Furthmuller, Phys. Rev. B **54**, 11169 (1996).
[24] O. Jepsen and O. K. Andersen, Z. Phys. B: Condens. Matter **97**, 35 (1995).